BMC Neuroscience

RESEARCH

Open Access

Evaluation of suitable reference genes for gene expression studies in the developing mouse cortex using RT-qPCR

Ananya Uppalapati[1†], Timothy Wang[1†] and Lena H. Nguyen[1*]

Abstract

Background Real-time quantitative PCR (RT-qPCR) is a widely used method to investigate gene expression in neuroscience studies. Accurate relative quantification of RT-qPCR requires the selection of reference genes that are stably expressed across the experimental conditions and tissues of interest. While RT-qPCR is often performed to investigate gene expression changes during neurodevelopment, few studies have examined the expression stability of commonly used reference genes in the developing mouse cortex.

Results Here, we evaluated the stability of five housekeeping genes, *Actb*, *Gapdh*, *B2m*, *Rpl13a*, and *Hprt*, in cortical tissue from mice at embryonic day 15 to postnatal day 0 to identify optimal reference genes with stable expression during late corticogenesis. The expression stability was assessed using five computational algorithms: BestKeeper, geNorm, NormFinder, DeltaCt, and RefFinder. Our results showed that *B2m*, *Gapdh*, and *Hprt*, or a combination of *B2m/Gapdh* and *B2m/Hprt*, were the most stably expressed genes or gene pairs. In contrast, *Actb* and *Rpl13a* were the least stably expressed.

Conclusion This study identifies *B2m*, *Gapdh*, and *Hprt* as suitable reference genes for relative quantification in RT-qPCR-based cortical development studies spanning the period of embryonic day 15 to postnatal day 0.

Keywords Cerebral cortex, Neurodevelopment, Mouse, RT-qPCR, Gene expression, Reference genes, Housekeeping genes

Introduction

The development of the mammalian cerebral cortex is a highly complex process that involves elaborate sequences of events governed by precise molecular signaling and gene expression. In mice, corticogenesis begins on embryonic day (E) 10, when neural progenitor cells begin to proliferate and differentiate [1]. This is followed by neuronal migration, which ultimately gives rise to the six cortical cell layers that underpin cognition and higher brain functions [2]. Pups are typically born on E19-21, and the cortical circuits continue to mature and refine after birth [3]. Although the processes of cortical development are well-described, the specific mechanisms

†Ananya Uppalapati and Timothy Wang contributed equally to this work.

*Correspondence:
Lena H. Nguyen
lena.nguyen@utdallas.edu
[1]Department of Neuroscience, School of Behavioral and Brain Sciences, The University of Texas at Dallas, Richardson, TX 75080, USA

of gene regulation in healthy development and disease are not fully understood and remain an active area of research.

Despite the emergence of high-throughput gene profiling technologies, such as microarrays and RNA sequencing, real-time quantitative PCR (RT-qPCR) remains a widely used method for highly sensitive and accurate mRNA quantification. RT-qPCR data is commonly analyzed using relative quantification methods, wherein the expression of a target gene is measured relative to a reference gene within that sample [4, 5]. For accurate normalization, the reference gene must be expressed at constant levels across experimental conditions. To this end, housekeeping genes are often used since they are essential for basic cellular functions and are presumed to be stably expressed across cells and conditions [6]. However, studies have shown that some housekeeping genes can change expression in response to various conditions [7], emphasizing the importance of validating the expression stability of reference genes in specific cell types, tissues, organisms, and conditions of interest. In neuroscience, such reference gene validation studies have been performed in rodent brain tissue from a wide range of conditions, including various brain diseases [8–16], injuries [17–22], tumors [23], stroke and hypoxia-ischemia [24–27], infection [28, 29], inflammation [30], drugs and alcohol exposure [31–33], toxin exposure [34–36], hormone therapy [37, 38], pregnancy and reproduction [39, 40], and diet [41–43]. Several studies have also assessed reference gene stabilities in the rodent brain during various embryonic and postnatal periods [44–49].

In this study, we evaluated the stability of five common housekeeping genes, β-actin (*Actb*), Glyceraldehyde-3-phosphate dehydrogenase (*Gapdh*), β2 microglobulin (*B2m*), Ribosomal protein L13a (*Rpl13a*), and Hypoxanthine–guanine phosphoribosyl transferase (*Hprt*) during late cortical development using RT-qPCR. Whereas early corticogenesis (E10-15) is associated with critical cell proliferation and peak neurogenesis, late corticogenesis (E15-P0) reflects an important time window for neuronal migration, maturation, and integration into cortical networks [1–3]. Disruption of these later developmental processes has been associated with many cognitive and neuropsychiatric disorders [50–54]. To identify stable reference genes that are suitable for RT-qPCR studies spanning late corticogenesis in mice, we assessed the expression stability of *Actb*, *Gapdh*, *B2m*, *Rpl13a*, and *Hprt* in cortical tissue from E15, E17, and postnatal day (P) 0 mice using five popular computational algorithms–BestKeeper [55], geNorm [56], NormFinder [57], DeltaCt [58], and RefFinder [59, 60]. Overall, we identified *B2m*, *Gapdh*, and *Hprt* as the most stably expressed genes, and *Actb* and *Rpl13a* as the least stably expressed genes, in E15 to P0 cortical tissue.

Methods

Animal tissue collection

All animal procedures were approved by The University of Texas at Dallas Institutional Animal Care and Use Committee (IACUC) and performed following the NIH Guide for the Care and Use of Laboratory Animals. All efforts were made to minimize suffering.

Three E14 time-pregnant CD-1 mice were purchased from Charles River Laboratories (USA) and housed in light-, temperature-, and humidity-controlled rooms on a 12:12 light/dark cycle. The dams were randomly assigned to either the E15, E17, or P0 groups, and cortical tissue from six littermate offspring was collected from each dam at the specified ages. For the E15 and E17 timepoints, pregnant mice were deeply anesthetized with isoflurane and decapitated. Embryos were removed from the abdominal cavity, and whole cortical hemispheres were rapidly dissected in ice-cold phosphate-buffered saline (PBS; 137mM NaCl, 2.7mM KCl, 10 mM Na_2HPO_4, 1.8mM KH_2PO_4, pH 7.4) under a stereomicroscope (Motic SMZ 1717). For the P0 timepoint, pups were anesthetized with isoflurane, decapitated, and whole cortical hemispheres were dissected as described above. Isolated tissues were immediately flash frozen in dry ice and stored at -80 °C until used. Each biological replicate consisted of one whole cortical hemisphere from an individual animal. All animals within each age group were from the same litter.

Total RNA isolation and quality control

Total RNA was extracted from whole cortical hemispheres using the RNeasy Plus Universal Mini Kit (Qiagen 73404) following the manufacturer's protocol. Tissues were homogenized using QIAzol Lysis Reagent by passing the tissue through a 27-gauge needle and syringe. Genomic DNA was removed using the gDNA Eliminator Solution included in the kit. Purified RNA was eluted from the spin column with 60 µl RNase-free water and stored at -80 °C.

Total RNA concentration and quality were measured using the NanoDrop One UV-vis spectrophotometer (Thermo Scientific). The RNA yields ranged from 12.0 to 15.9 µg (E15), 15.9–26.1 µg (E17), and 34.7–52.7 µg (P0). The A260/A280 absorbance ratios were 2.0-2.2 and the A260/A230 ratios were 0.4–2.3 for all samples. The lower-than-expected A260/A230 values were found in some of the E15 and E17 samples due to trace presence of guanidinium thiocyanate from the extraction reagents. In these samples, the guanidinium thiocyanate was present at a concentration of < 15 mM. Per the RNA extraction kit manufacturer's guidelines, guanidine thiocyanate concentrations of < 100 mM in RNA samples are not thought to compromise RT-qPCR reliability (https://www.qiagen.com/us/resources/faq?id=c59936fb-4f1e-4191-9c16-ff08

3cb24574%26;lang=en), and therefore, the samples were deemed acceptable for downstream experiments. RNA integrity was assessed by denaturing agarose gel electrophoresis. The RNA samples were run on a 1% agarose gel stained with ethidium bromide and visualized using the ChemiDoc Imaging System (Bio-Rad). All samples displayed sharp 28 S and 18 S ribosomal RNA bands, indicating intact RNA.

cDNA synthesis

First-strand cDNA synthesis was performed using the iScript gDNA Clear cDNA Synthesis Kit (Bio-Rad 172–5034) following the manufacturer's protocol. For each sample, 500 ng total RNA was treated with the kit's DNase reagent, followed by incubation at 25 °C for 5 min (DNA digestion) and 75 °C for 5 min (DNase inactivation) to eliminate genomic DNA. DNAse-treated RNA samples were then converted to cDNA using the iScript Reverse Transcription Supermix (or the iScript no-Reverse Transcription Supermix for no reverse transcription controls). cDNA synthesis was performed on a PT100 thermocycler (Bio-Rad) using the following thermal protocol: 25 °C for 5 min (priming), 46 °C for 20 min (reverse transcription), and 95 °C for 1 min (reverse transcription inactivation). The cDNA samples were stored at -20 °C.

Real-time quantitative PCR (RT-qPCR)

RT-qPCR was performed using 96-well PrimePCR Custom Plates (Bio-Rad 10025216). Each plate contained pre-designed PrimePCR primer assays for 5 housekeeping genes: *Actb*, *Gapdh*, *B2m*, *Rpl13a*, and *Hprt*. The primers were previously tested and validated for amplification specificity, efficiency, linear dynamic range, and background signal by the manufacturer to meet the Minimum Information for Publication of Quantitative Real-Time PCR Experiments (MIQE) guidelines [61]. The list of evaluated candidate reference genes and primer characteristics are listed in Table 1.

The RT-qPCR reactions were carried out using the SsoAdvanced Universal SYBR Green Supermix (Bio-Rad 172–5270), which contains the antibody-mediated hot-start Sso7d fusion polymerase and optimized buffers for maximum efficiency and sensitivity, following the manufacturer's protocol. Each reaction contained 15 ng cDNA (equivalent to 3% input RNA) in a 20 µl reaction volume. RT-qPCR was performed on a CFX Duet Real-Time PCR System (Bio-Rad) using the following thermal protocol: 95 °C for 2 min (activation), followed by 40 cycles of 95 °C for 5 s (denaturation) and 60 °C for 30 s (annealing/extension). A final melting curve protocol was performed for all plate runs: 95 °C for 5 s, followed by an increase from 65 °C to 95 °C at 0.5 °C increments in 5 s.

The experiment was run on two 96-well plates. Each plate contained 3 biological replicates (i.e., 3 mice) per age group with 2 technical replicates per biological replicate (final sample number $n = 6$ mice per group). No reverse transcription and no template controls were included for all experiments.

Data analysis and statistics

The qPCR amplification curves, melting curves, and Ct values were analyzed with the CFX Maestro software (Bio-Rad) and imported into Microsoft Excel. The Ct values for each biological replicate (i.e., each mouse) were obtained by averaging the values from the two technical replicates. The Ct and standard deviation (SD) data were organized into all samples combined and as separate age groups for each gene (Table 2). Differences in Ct values between the age groups were analyzed by one-way ANOVA with Tukey's post-hoc test using GraphPad Prism 10 software. The significance value was set at $p < 0.05$.

Gene expression stability analyses were performed by inputting raw Ct values into the web-based RefFinder

Table 1 List of candidate reference genes and primer characteristics

Gene symbol	Gene name	Function	UniGene ID	Assay ID	Assay design	Amplicon size (bp)	Amplification efficiency (%)
Actb	β-actin	Cytoskeletal structural protein	Mm.391967	qMmuCED0027505	Exonic	109	101
Gapdh	Glyceraldehyde-3-phosphate dehydrogenase	Glycolysis enzyme	Mm.304088	qMmuCED0027497	Exonic	75	101
B2m	β2 microglobulin	Component of major histocompatibility complex (MHC) class I molecules	Mm.163	qMmuCID0040553	Intron-spanning	112	100
Rpl13a	Ribosomal protein L13A	Ribosome component; protein synthesis	Mm.180458	qMmuCED0040629	Exonic	70	90
Hprt	Hypoxanthine-guanine phosphoribosyl transferase	Purine synthesis in salvage pathways	Mm.299381	qMmuCID0005679	Intron-spanning	70	94

Table 2 Mean Ct values and standard deviation of candidate reference genes

		Mean Ct	SD	*n*
Actb	All combined	18.99	1.14	18
	E15	18.97	1.05	6
	E17	18.93	1.35	6
	P0	19.07	1.22	6
Gapdh	All combined	20.58	0.86	18
	E15	20.52	0.74	6
	E17	20.57	1.05	6
	P0	20.66	0.9	6
B2m	All combined	26.01	0.58	18
	E15	25.78	0.35	6
	E17	26.01	0.75	6
	P0	26.23	0.56	6
Rpl13a	All combined	19.58	0.53	18
	E15	19.21	0.41	6
	E17	19.58	0.5	6
	P0	19.96	0.44	6
Hprt	All combined	25.07	0.61	18
	E15	25.26	0.52	6
	E17	25.12	0.71	6
	P0	24.82	0.59	6

SD, standard deviation; n, sample size

tool (https://www.ciidirsinaloa.com.mx/RefFinder-master/). RefFinder performs stability analysis using the BestKeeper [55], geNorm [56], NormFinder [57], and DeltaCt [58] algorithms and provides a comprehensive stability ranking based on the geometric mean of the ranks from each program. Data generated by RefFinder were individually confirmed using the following Excel-based tools for each specific program: BestKeeper v1.0 (https://www.gene-quantification.de/bestkeeper.html), GeNorm v3 (https://genorm.cmgg.be), and NormFinder v0953 (https://www.moma.dk/software/normfinder). RefFinder's DeltaCt results were manually calculated and confirmed using Excel. All data were analyzed at 100% amplification efficiency. The algorithmic basis and criteria for ranking in each program are further explained in the Results.

Results

Selection of candidate reference genes, qPCR amplification, and primer specificity

The five candidate reference genes in this study were chosen based on their cellular functions and popular use in neuroscience research. We selected housekeeping genes with different functional classes, including cytoskeleton structure (*Actb*), metabolism (*Gapdh*, *Hprt*), major histocompatibility complex class I component (*B2m*), and protein synthesis (*Rpl13a*), to diversify the list of candidate reference genes and to minimize the chance that the evaluated genes are co-regulated (see Table 1).

All evaluated genes amplified with Ct values between 17 and 28 across all samples (Table 2; see Supplementary Fig. 1a, c for amplification curves). Melt curve analyses revealed single peaks for all PCR reactions at the expected primer melting temperatures, indicating the presence of single amplicons in the reactions (Supplementary Fig. 1b, d). No amplifications were detected in the no reverse transcription and no template controls, verifying the absence of genomic DNA contamination and non-specific amplification. The raw Ct values for all samples and negative controls are available in Supplementary Tables 1–4.

Ct values for candidate reference genes

To examine the expression levels of the selected genes, we evaluated the Ct values for each gene in the combined E15, E17, and P0 age groups (Fig. 1a; Table 2). The mean Ct values ranged from 18.99 to 26.01, verifying abundant target gene expression in the cortical tissue samples. Among these genes, *Actb* (mean Ct = 18.99), *Gapdh* (mean Ct = 20.58), and *Rpl13a* (mean Ct = 19.58) were the most abundant, while *B2m* (mean Ct = 26.01) and *Hprt* (mean Ct = 25.07) were the least abundant (Fig. 1a; Table 2). *Rpl13a* had the smallest expression level variation (SD = 0.53) with a maximum difference of 2 cycles across samples, while *Actb* had the largest variation (SD = 1.14) with a maximum difference of 3.5 cycles across samples (Fig. 1a; Table 2).

To test whether the mean Ct values were different between age groups, we separated the data according to age and performed a one-way ANOVA with Tukey's post-hoc test to assess group differences (Fig. 1b; Table 2). We found a small but significant increase in the mean Ct values of *Rpl13a* between E15 and P0 [$F(2, 15) = 4.1720$, $p = 0.0363$, Tukey's post-hoc test: $p < 0.05$, Fig. 1b]. No significant age-dependent changes were observed in the other genes [*Actb*: $F(2, 15) = 0.0231$, $p = 0.9772$, *Gapdh*: $F(2, 15) = 0.0354$, $p = 0.9653$, *B2m*: $F(2, 15) = 0.8920$, $p = 0.4305$, *Hprt*: $F(2, 15) = 0.8154$, $p = 0.4612$, Fig. 1b].

Expression stability of candidate reference genes

To determine the expression stability of the candidate reference genes, we applied the BestKeeper, geNorm, NormFinder, DeltaCt, and RefFinder algorithms. These algorithms calculate an expression stability measure based on Ct values and rank each gene from least to most stable based on the measures. The stability ranking results from each program are plotted in Fig. 2.

BestKeeper calculates a set of descriptive statistics, including the arithmetic mean Ct, the geometric mean Ct, the minimal and maximal Ct values, the mean absolute deviation (MAD) from the arithmetic mean, and the coefficients of variance for each candidate reference gene [55]. The extreme values of over- or under-expression levels, expressed as minimum or maximum x-fold compared to the geometric mean Ct, and the x-fold

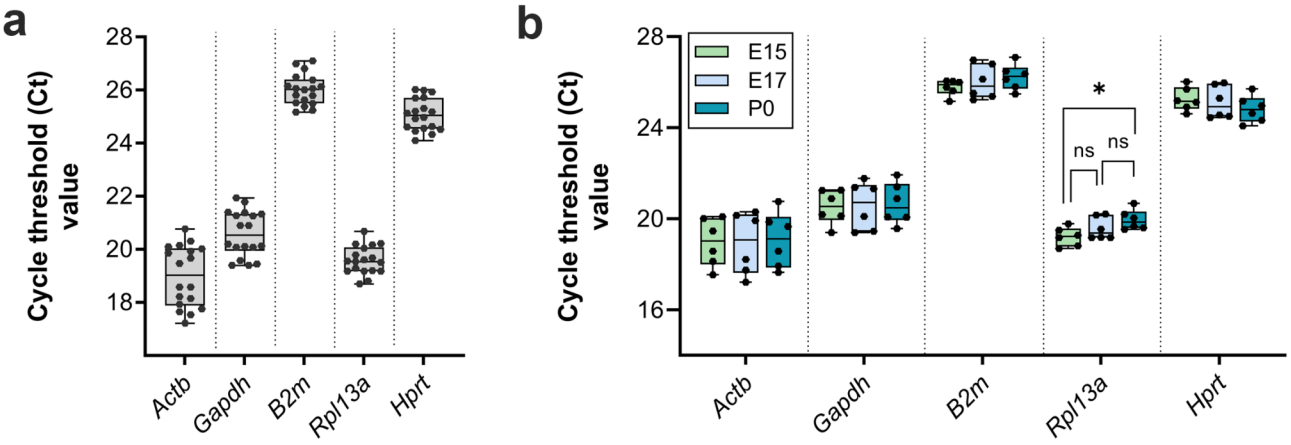

Fig. 1 Cycle threshold (Ct) values of candidate reference genes in E15 to P0 mouse cortical tissue. (**a**) Box-and-whisker plot showing the distribution of Ct values for candidate reference genes in the combined age groups. $n = 18$ mice per gene. (**b**) Box-and-whisker plot showing Ct values of candidate reference genes in the individual age groups. $n = 6$ mice per age group. For each candidate gene, the differences in Ct values between the age groups were analyzed by one-way ANOVA. Where the ANOVA was significant, a Tukey's post-hoc test was applied. Significant Tukey's pairwise comparisons are denoted with a star: $^*p < 0.05$ (*Rpl13a* E15 vs. P0). The line inside the box indicates the median, the boxes represent the 25th and 75th percentiles, and the whiskers show the minimum and maximum values. The dots represent values from individual animals. *Ct*, *cycle threshold*

absolute deviation are also calculated. The descriptive statistics of the current dataset are listed in Table 3. BestKeeper uses MAD to rank the genes from the most to least stable expression. Genes with lower MAD have higher stability, whereas those with MAD > 1 are unstable [55]. By this approach, the most stable gene was *Rpl13a* (MAD = 0.413), followed by *B2m* (MAD = 0.452), *Hprt* (MAD = 0.503), and *Gapdh* (MAD = 0.762). *Actb* had a MAD of 1.034 and was considered unstable (Fig. 2a).

geNorm calculates a stability measure (M value) based on the principle that two ideal reference genes should have identical expression ratios in all samples, regardless of experimental conditions or tissue type [56]. For each candidate reference gene, the pairwise variation (as determined by the SD of logarithmically transformed expression ratios) between that gene and other tested genes is calculated, and the stability value, M, is determined based on the average pairwise variations. A lower M value indicates greater stability. Stepwise exclusion of the least stable gene (i.e., highest M value) is iteratively performed to rank the tested genes until the two most stable genes are identified. An M value of ≤ 1.5 indicates stable expression, although stably expressed genes usually display an M value < 0.5. Based on this analysis, *B2m* and *Rpl13a* were identified as the two most stable genes (M = 0.293), followed by *Hprt* (M = 0.423) and *Gapdh* (M = 0.456). *Actb* was the least stable gene (M = 0.529) (Fig. 2b).

NormFinder calculates a stability value (S) for each candidate reference gene based on a mathematical model that estimates both the inter- and intra-group expression variation of candidate reference genes in a sample set [57]. When the sample set was analyzed as one group (i.e., without group identifiers), *Gapdh* was the most stable gene (S = 0.159), followed by *B2m* (S = 0.202), *Hprt* (S = 0.355), and *Rpl13a* (S = 0.494). *Actb* was the least stable gene (S = 0.580) (Fig. 2c). When both inter- and intra-group variations were considered, *Gapdh* (S = 0.125) and *B2m* (S = 0.157) remained the two most stable genes, followed by *Hprt* (S = 0.282) and *Actb* (S = 0.306). *Rpl13a* (S = 0.309) was the least stable gene, consistent with the observations that the mean Ct significantly increases between E15 and P0 (Fig. 2d). Studies have suggested using a combination of reference genes rather than a single reference gene for more robust target gene normalization [56]. To this end, NormFinder also calculates a combined stability value for each gene pair to determine the combination of two genes with the highest stability [57]. Here, *Gapdh* and *B2m* were identified as the gene combination with the highest combined stability value (S = 0.11), followed by *B2m* and *Hprt* (S = 0.16) (Table 4).

DeltaCt selects the most stable reference genes by comparing the relative expression (delta Ct) of pairs of genes within a tissue sample [58]. For each candidate reference gene, the mean SD (SD_{avg}) derived from a set of pairwise comparisons between the candidate gene and other tested genes is used to rank stability. Genes with lower SD_{avg} are considered more stable. By this method, the most stable genes were *Gapdh* (SD_{avg} = 0.451) and *B2m* (SD_{avg} = 0.451), followed by *Hprt* (SD_{avg} = 0.527) and *Rpl13a* (SD_{avg} = 0.560). *Actb* had the lowest stability (SD_{avg} = 0.639) (Fig. 2e).

To incorporate all the results from Bestkeeper, geNorm, NormFinder, and DeltaCt, we performed a final comprehensive ranking using RefFinder [59, 60]. The RefFinder algorithm compares the rankings from the four aforementioned programs and assigns an appropriate weight to each gene. The geometric mean of their

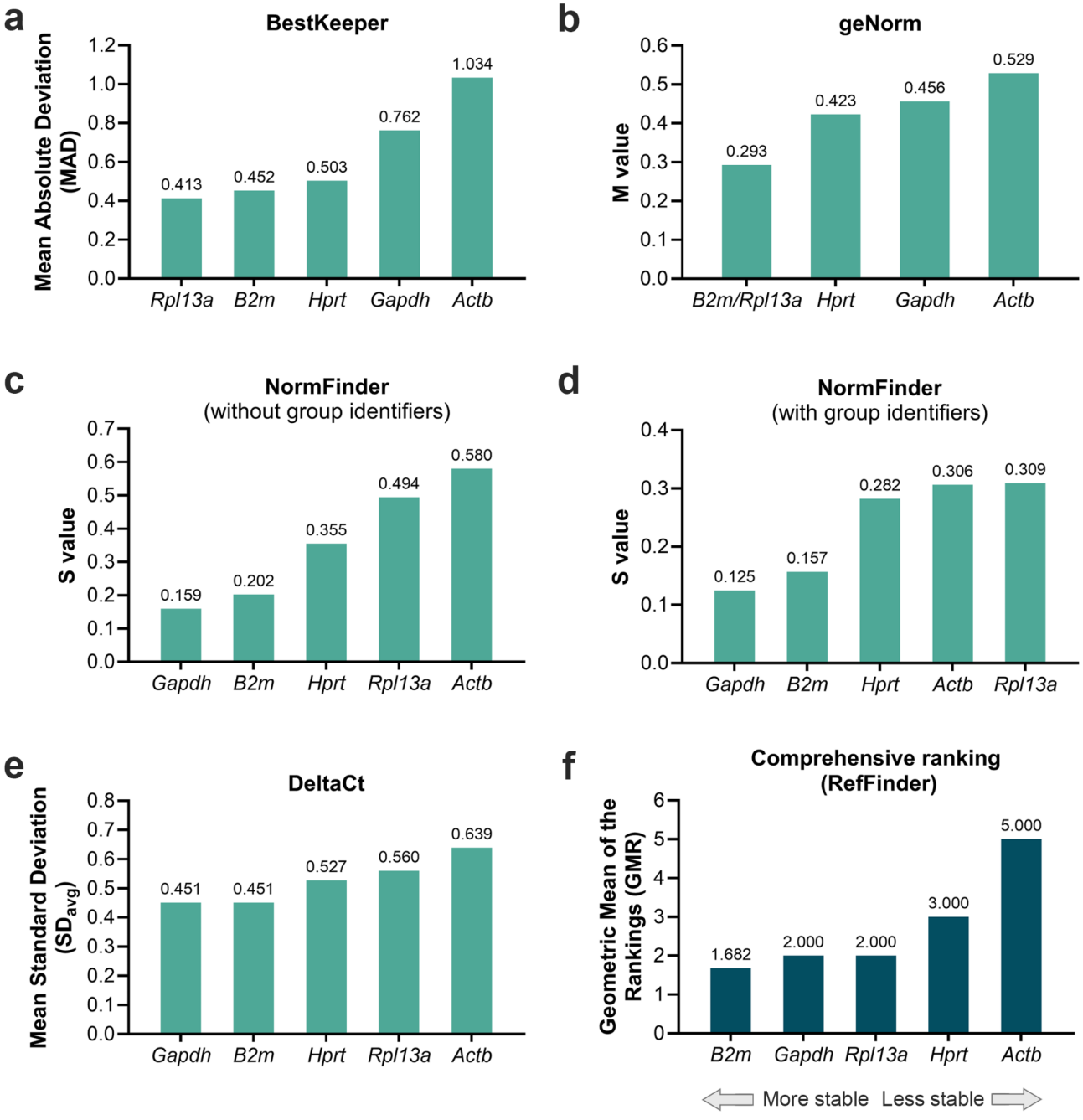

Fig. 2 Stability rankings according to BestKeeper, geNorm, NormFinder, DeltaCt, and RefFinder. Bar graphs showing gene expression stability rankings according to (**a**) BestKeeper, (**b**) geNorm, (**c**) NormFinder (without group identifiers), (**d**) NormFinder (with group identifiers), (**e**) DeltaCt, and (**f**) RefFinder. Genes are organized from the most to least stable. The stability values for each gene as calculated by each algorithm are shown on top of the bars. *MAD, average absolute deviation; M value, stability measure; S value, stability value;* SD_{avg}*, mean standard deviation; GMR, geometric mean of the rankings*

rankings (GMR) is then calculated and an overall ranking is provided. Genes with lower GMR have more stable expression. Using this integrated approach, *B2m* was identified as the most stable gene (GMR = 1.682), followed by equally ranked *Gapdh* (GMR = 2.000) and *Rpl13a* (GMR = 2.000), and *Hprt* (GMR = 3.000). *Actb* was identified as the least stable gene (GMR = 5.000), consistent with the results from the individual programs (Fig. 2f). The expression stability values and rankings according to each algorithm are summarized in Table 5.

Discussion

In this study, we evaluated the suitability of *Actb*, *Gapdh*, *B2m*, *Rpl13a*, and *Hprt* as reference genes in E15 to P0 mouse cortical tissue samples using RT-qPCR and computational algorithms to analyze expression stability. We

Table 3 Ct descriptive statistics obtained by BestKeeper

	Actin	*Gapdh*	*B2m*	*Rpl13a*	*Hprt*
Arithmetic mean (Ct)	18.99	20.58	26.01	19.58	25.07
Geometric mean (Ct)	18.96	20.57	26.00	19.57	25.06
Min (Ct)	17.22	19.39	25.16	18.69	24.09
Max (Ct)	20.76	21.93	27.09	20.68	26.02
MAD (± Ct)	1.034	0.762	0.452	0.413	0.503
CV (% Ct)	5.44	3.70	1.74	2.11	2.01
Min (x-fold)	-3.34	-2.26	-1.79	-1.84	-1.96
Max (x-fold)	3.49	2.58	2.13	2.16	1.95
MAD (± x-fold)	2.05	1.70	1.37	1.33	1.42
n	18	18	18	18	18

Min, minimum; Max, maximum; MAD, average absolute deviation; CV, coefficient of variance; n, sample size

Table 4 Combined stability values of gene pairs obtained by NormFinder

Gene combination	Stability value
Actb/Gapdh	0.18
Actb/B2m	0.19
Actb/Hprt	0.29
Gapdh/B2m	0.11
Gapdh/Hprt	0.21
B2m/Hprt	0.16

found that *B2m*, *Gapdh*, and *Hprt*, or a combination of *B2m/Gapdh* and *B2m/Hprt*, had the highest expression stability in the cortex during the period of E15 to P0, and we recommend them as reliable reference genes for studying mouse late corticogenesis. We caution against using *Actb* and do not recommend using *Rpl13a* due to low stability and high expression variability.

Several computational algorithms have been developed to identify optimal reference genes based on non-normalized expression stability rankings, including BestKeeper [55], geNorm [56], NormFinder [57], and DeltaCt [58]. The underlying principle of these programs is that genes with the most stable expression across samples and conditions are the best references. However, due to differences in methodologies, these algorithms may produce different stability rankings. Therefore, a newer fifth algorithm, RefFinder, was developed to reconcile the differences by providing a comprehensive ranking based on the geometric mean of weighted rankings from the previous algorithms [59, 60]. In the present study, RefFinder identified *B2m* as the most stable gene among the evaluated genes, followed by equally ranked *Gapdh* and *Rpl13a*, and then *Hprt*. *B2m* was consistently ranked in the top two genes across all algorithms. *Gapdh* was ranked the most stable gene by NormFinder and DeltaCt, but second to lowest by BestKeeper and GeNorm. Conversely, *Rpl13a* was ranked the highest by BestKeeper and geNorm, but second to lowest by NormFinder and DeltaCt. These discrepancies can be explained by the algorithmic differences and ranking criteria used by each

Table 5 Stability values and rankings according to BestKeeper, geNorm, NormFinder, DeltaCt, and RefFinder

Gene	BestKeeper		geNorm		NormFinder (without group identifiers)		NormFinder (with group identifiers)		DeltaCt		Comprehensive ranking (RefFinder)	
	MAD	Rank	M value	Rank	S value	Rank	S value	Rank	SD_{avg}	Rank	GMR	Rank
Actb	1.034	5	0.529	5	0.580	5	0.306	4	0.639	5	5.000	5
Gapdh	0.762	4	0.456	4	0.159	1	0.125	1	0.451	1	2.000	2
B2m	0.452	2	0.293	1	0.202	2	0.157	2	0.451	2	1.682	1
Rpl13a	0.413	1	0.293	1	0.494	4	0.309	5	0.560	4	2.000	2
Hprt	0.503	3	0.423	3	0.355	3	0.282	3	0.527	3	3.000	4

MAD, average absolute deviation; M value, stability measure; S value, stability value; SD_{avg}, mean standard deviation; GMR, geometric mean of the ranking

program. For example, geNorm prioritizes the pairwise variation of a particular gene with all the other candidate genes, whereas NormFinder uses a model-based approach to estimate the expression variation of each gene independently of the other genes [56, 57]. These program-specific differences further emphasize the utility of RefFinder. When both the inter- and intra-group variances were considered in NormFinder, *Rpl13a* was ranked the least stable, consistent with our data showing significant differences in the mean Ct values between E15 and P0. The age-dependent differences in *Rpl13a* expression suggest that it is developmentally regulated and thus not an appropriate reference for target gene normalization in cortical development studies. *Actb* was consistently ranked the lowest in all algorithms and did not meet, albeit barely, the cutoff value for stable genes by BestKeeper criteria. Although *Actb* stability values were within the range for stable genes using the other algorithms, we suggest using alternate genes that are more stably expressed. Taking into consideration the results from multiple stability ranking algorithms, we propose using *B2m*, *Gapdh*, and *Hprt*, or a combination of *B2m/Gapdh* or *B2m/Hprt*, as reference genes for RT-qPCR in mouse cortical samples spanning late corticogenesis.

Our study re-emphasizes the importance of validating reference genes in both the specific tissues and developmental stages of interest. In a previous developmental study using whole brain tissue from earlier mouse embryonic stages (E11 to E15), *Actb* was ranked the third most stable gene out of ten evaluated genes, whereas *Gapdh* was in sixth place [45]. This is in contrast to our findings in E15 to P0 cortex-specific samples where *Gapdh* was among the most stable gene and *Actb* was the least stable. Studies across different developmental windows in other brain regions and nervous system tissues have also reported different stability rankings for the genes we assessed [47]. To our knowledge, only one previous study has examined the stability of reference genes specifically in mouse cortical tissue during embryonic development by RT-qPCR [44]. In this study, the authors used various descriptive statistics to examine the stability of *Actb*, *Gapdh*, and *Hprt*, as well as ribosomal protein 18s (*18s*) and RNA polymerase II (*RpII*), across nine developmental stages between E10 and P56 in C57BL/6 mice. In their sample set, *Gapdh* was consistently ranked the most stable gene, *Hprt* was ranked in the middle, and *Actb* was ranked the lowest. In the present study, we applied several computational algorithms to analyze reference gene expression stabilities in the period of late corticogenesis (E15-P0) in CD-1 mice. Our results with regards to *Gapdh*, *Hprt*, and *Actb* stabilities corroborate the former study, highlighting a consistency in the results across mouse strain backgrounds. Additionally, we identified *B2m* as a reliable reference gene for late corticogenesis studies. This provides more options for reference gene selection, considering optimal references should have Ct values as close as possible to that of the target gene to ensure accurate quantification [62].

The most stable gene in our data set, *B2m*, encodes for β2 microglobulin, a subunit of the major histocompatibility complex class I (MHC-I) [63]. Recent studies have shown that β2 microglobulin plays crucial roles in several neurological disorders, however, the role in cortical development is not well understood [63]. The second most stable genes, *Gapdh* and *Hprt*, encode enzymes that participate in crucial metabolic pathways, including glycolysis and purine salvaging, respectively [64, 65]. Our findings suggest that these genes are consistently expressed to support these vital processes during late corticogenesis. The lowest-ranked gene, *Actb*, encodes for β-actin, which is a structural protein that is an essential component of the cytoskeleton [66]. The period between E15 and P0 reflects a time window when substantial cell migration events and morphogenesis are occurring. These processes require dynamic cytoskeletal changes, which may explain the lowered *Actb* expression stability during this period. Unlike the other evaluated genes, *Rpl13a* displayed a small albeit significant decrease in expression between E15 and P0, suggesting its expression is developmental stage-dependent. *Rpl13a* encodes for a ribosomal subunit that is involved in the regulation of mRNA translation and protein synthesis [67]. The observed decrease in *Rpl13a* expression is consistent with studies demonstrating a developmental shift in the cortical ribosome signature between E15 and E18 that includes downregulation of multiple ribosomal proteins [68, 69]. These ribosome changes are thought to contribute to the dynamic gene regulatory mechanisms that drive the spatiotemporal development of the cortex, though the specific function of *Rpl13a* in cortical development is unknown.

Finally, there are several limitations to our study. Here, we only tested five genes for their reliability as references in cortical tissue from E15 to P0, and other yet-to-be-evaluated housekeeping genes may also be suitable for this purpose. Furthermore, we did not assess the impact of sex on gene stability, but this should be considered for sex-dimorphic development studies since it has been reported that housekeeping gene stability can vary between males and females during brain development [45]. Lastly, our study analyzed total RNA from whole cortical lysates and does not account for cell type-specific gene expression. Given the numerous cell types that are present during the final stages of corticogenesis (e.g., pyramidal neurons, interneurons, and glia), single-cell transcriptomic studies during mouse cortical development, such as those by Loo et al. [70] and Di Bella et

al. [71], will be useful to understand gene expression in single cell types.

Conclusions

In conclusion, our result supports the stable expression of *B2m*, *Gapdh*, and *Hprt* in the mouse cortex during the period of E15 to P0, and we recommend using *B2m*, *Gapdh*, and *Hprt* or a combination of *B2m/Gapdh* and *B2m/Hprt* as reliable RT-qPCR reference genes for studying mouse late corticogenesis. We caution against using *Actb* due to lower expression stability and do not recommend using *Rpl13a* since its expression changes with developmental stage. The differences in expression stabilities of known housekeeping genes during cortical development may reflect their distinct roles in developmental processes and further underscore the importance of validating the expression stability of reference genes for the experimental tissue and conditions of interest.

Supplementary Information

The online version contains supplementary material available at https://doi.org/10.1186/s12868-025-00934-y.

Supplementary Material 1

Acknowledgements
Not applicable.

Author contributions
AU and TW collected and analyzed the data. LN designed the study, analyzed the data, and wrote the manuscript. All authors read and approved the final manuscript.

Funding
Not applicable.

Data availability
All data generated or analyzed during this study are included in this published article and its supplementary information files.

Declarations

Ethical approval
All animal procedures were approved by The University of Texas at Dallas Institutional Animal Care and Use Committee (IACUC) and performed following the NIH Guide for the Care and Use of Laboratory Animals.

Consent for publication
Not applicable.

Competing interests
The authors declare no competing interests.

Received: 13 August 2024 / Accepted: 6 February 2025
Published online: 18 February 2025

References

1. Mukhtar T, Taylor V. Untangling cortical complexity during development. J Exp Neurosci. 2018;12:1179069518759332.
2. Buchsbaum IY, Cappello S. Neuronal migration in the CNS during development and disease: insights from in vivo and in vitro models. Development. 2019;146(1).
3. Zeiss CJ. Comparative milestones in Rodent and human postnatal Central Nervous System Development. Toxicol Pathol. 2021;49(8):1368–73.
4. Schmittgen TD, Livak KJ. Analyzing real-time PCR data by the comparative C(T) method. Nat Protoc. 2008;3(6):1101–8.
5. Livak KJ, Schmittgen TD. Analysis of relative gene expression data using real-time quantitative PCR and the 2(-Delta Delta C(T)) method. Methods. 2001;25(4):402–8.
6. Joshi CJ, Ke W, Drangowska-Way A, O'Rourke EJ, Lewis NE. What are housekeeping genes? PLoS Comput Biol. 2022;18(7):e1010295.
7. Thellin O, Zorzi W, Lakaye B, De Borman B, Coumans B, Hennen G, Grisar T, Igout A, Heinen E. Housekeeping genes as internal standards: use and limits. J Biotechnol. 1999;75(2–3):291–5.
8. Pernot F, Dorandeu F, Beaup C, Peinnequin A. Selection of reference genes for real-time quantitative reverse transcription-polymerase chain reaction in hippocampal structure in a murine model of temporal lobe epilepsy with focal seizures. J Neurosci Res. 2010;88(5):1000–8.
9. Swijsen A, Nelissen K, Janssen D, Rigo JM, Hoogland G. Validation of reference genes for quantitative real-time PCR studies in the dentate gyrus after experimental febrile seizures. BMC Res Notes. 2012;5:685.
10. de Araujo MA, Marques TE, Taniele-Silva J, Souza FM, de Andrade TG, Garcia-Cairasco N, Paco-Larson ML, Gitai DL. Identification of endogenous reference genes for the analysis of microRNA expression in the hippocampus of the pilocarpine-induced model of mesial temporal lobe epilepsy. PLoS ONE. 2014;9(6):e100529.
11. Crans RAJ, Janssens J, Daelemans S, Wouters E, Raedt R, Van Dam D, De Deyn PP, Van Craenenbroeck K, Stove CP. The validation of short Interspersed Nuclear Elements (SINEs) as a RT-qPCR normalization strategy in a rodent model for temporal lobe epilepsy. PLoS ONE. 2019;14(1):e0210567.
12. Schwarz AP, Kovalenko AA, Malygina DA, Postnikova TY, Zubareva OE, Zaitsev AV. Reference Gene Validation in the Brain Regions of Young Rats after Pentylenetetrazole-Induced Seizures. Biomedicines. 2020;8(8).
13. Janssens J, Crans RAJ, Van Craenenbroeck K, Vandesompele J, Stove CP, Van Dam D, De Deyn PP. Evaluating the applicability of mouse SINEs as an alternative normalization approach for RT-qPCR in brain tissue of the APP23 model for Alzheimer's disease. J Neurosci Methods. 2019;320:128–37.
14. Zhou J, Zhang X, Ren J, Wang P, Zhang J, Wei Z, Tian Y. Validation of reference genes for quantitative real-time PCR in valproic acid rat models of autism. Mol Biol Rep. 2016;43(8):837–47.
15. Kummerfeld DM, Skryabin BV, Brosius J, Vakhrushev SY, Rozhdestvensky TS. Reference genes across nine brain areas of wild type and prader-Willi Syndrome mice: assessing differences in Igfbp7, Pcsk1, Nhlh2 and Nlgn3 expression. Int J Mol Sci. 2022;23(15).
16. Crawford AH, Hildyard JCW, Wells DJ, Piercy RJ. Identification of quantitative polymerase chain reaction reference genes suitable for normalising gene expression in the brain of normal and dystrophic mice and dogs. Wellcome Open Res. 2021;6:84.
17. Rhinn H, Marchand-Leroux C, Croci N, Plotkine M, Scherman D, Escriou V. Housekeeping while brain's storming validation of normalizing factors for gene expression studies in a murine model of traumatic brain injury. BMC Mol Biol. 2008;9:62.
18. Cook NL, Vink R, Donkin JJ, van den Heuvel C. Validation of reference genes for normalization of real-time quantitative RT-PCR data in traumatic brain injury. J Neurosci Res. 2009;87(1):34–41.
19. Harris JL, Reeves TM, Phillips LL. Injury modality, survival interval, and sample region are critical determinants of qRT-PCR reference gene selection during long-term recovery from brain trauma. J Neurotrauma. 2009;26(10):1669–81.
20. Timaru-Kast R, Herbig EL, Luh C, Engelhard K, Thal SC. Influence of age on cerebral housekeeping gene expression for normalization of quantitative polymerase chain reaction after Acute Brain Injury in mice. J Neurotrauma. 2015;32(22):1777–88.
21. Zamani A, Powell KL, May A, Semple BD. Validation of reference genes for gene expression analysis following experimental traumatic brain injury in a pediatric mouse model. Brain Res Bull. 2020;156:43–9.
22. Schlaudraff J, Paul MH, Deller T, Del Turco D. Precise measurement of gene expression changes in mouse brain areas denervated by injury. Sci Rep. 2022;12(1):22530.
23. van Rijn SJ, Riemers FM, van den Heuvel D, Wolfswinkel J, Hofland L, Meij BP, Penning LC. Expression stability of reference genes for quantitative RT-PCR of

healthy and diseased pituitary tissue samples varies between humans, mice, and dogs. Mol Neurobiol. 2014;49(2):893–9.
24. Kang Y, Wu Z, Cai D, Lu B. Evaluation of reference genes for gene expression studies in mouse and N2a cell ischemic stroke models using quantitative real-time PCR. BMC Neurosci. 2018;19(1):3.
25. Sieber MW, Guenther M, Kohl M, Witte OW, Claus RA, Frahm C. Inter-age variability of bona fide unvaried transcripts normalization of quantitative PCR data in ischemic stroke. Neurobiol Aging. 2010;31(4):654–64.
26. Pomierny B, Krzyzanowska W, Jurczyk J, Strach B, Skorkowska A, Leonovich I, Budziszewska B, Pera J. Identification of optimal reference genes for gene expression studies in a focal cerebral ischaemia model-spatiotemporal effects. J Cell Mol Med. 2022;26(10):3060–7.
27. Bustelo M, Bruno MA, Loidl CF, Rey-Funes M, Steinbusch HWM, Gavilanes AWD, van den Hove DLA. Statistical differences resulting from selection of stable reference genes after hypoxia and hypothermia in the neonatal rat brain. PLoS ONE. 2020;15(5):e0233387.
28. Mao Q, Zhang L, Guo Y, Sun L, Liu S, He P, Huang R, Sun L, Chen S, Zhang H, et al. Identification of suitable reference genes for BDV-infected primary rat hippocampal neurons. Mol Med Rep. 2016;14(6):5587–94.
29. Zhang L, Liu S, Zhang L, You H, Huang R, Sun L, He P, Chen S, Zhang H, Xie P. Real-time qPCR identifies suitable reference genes for Borna Disease virus-infected rat cortical neurons. Int J Mol Sci. 2014;15(12):21825–39.
30. Walder RY, Wattiez AS, White SR, Marquez de Prado B, Hamity MV, Hammond DL. Validation of four reference genes for quantitative mRNA expression studies in a rat model of inflammatory injury. Mol Pain. 2014;10:55.
31. He Y, Yu S, Bae E, Shen H, Wang Y. Methamphetamine alters reference gene expression in Nigra and striatum of adult rat brain. Neurotoxicology. 2013;39:138–45.
32. Taki FA, Abdel-Rahman AA, Zhang B. A comprehensive approach to identify reliable reference gene candidates to investigate the link between alcoholism and endocrinology in Sprague-Dawley rats. PLoS ONE. 2014;9(5):e94311.
33. Zhang Q, Zhang M, Li J, Xiao H, Wu D, Guo Q, Zhang Y, Wang H, Li S, Liao S. Selection and validation of reference genes for RT-PCR expression analysis of candidate genes involved in Morphine-Induced Conditioned Place Preference mice. J Mol Neurosci. 2018;66(4):587–94.
34. Bonefeld BE, Elfving B, Wegener G. Reference genes for normalization: a study of rat brain tissue. Synapse. 2008;62(4):302–9.
35. Ramhoj L, Axelstad M, Svingen T. Validation of endogenous reference genes in rat cerebral cortex for RT-qPCR analyses in developmental toxicity studies. PeerJ. 2019;7:e7181.
36. Nadei OV, Agalakova NI. Optimal reference genes for RT-qPCR experiments in Hippocampus and cortex of rats chronically exposed to excessive fluoride. Biol Trace Elem Res. 2024;202(1):199–209.
37. Gholami K, Loh SY, Salleh N, Lam SK, Hoe SZ. Selection of suitable endogenous reference genes for qPCR in kidney and hypothalamus of rats under testosterone influence. PLoS ONE. 2017;12(6):e0176368.
38. Feria-Romero IA, Bribiesca-Cruz I, Coyoy-Salgado A, Segura-Uribe JJ, Bautista-Poblet G, Granados-Cervantes A, Guerra-Araiza C. Validation of housekeeping genes as an internal control for gene expression studies in the brain of ovariectomized rats treated with tibolone. Gene. 2021;769:145255.
39. Berruien NNA, Murray JF, Smith CL. Pregnancy influences the selection of appropriate reference genes in mouse tissue: determination of appropriate reference genes for quantitative reverse transcription PCR studies in tissues from the female mouse reproductive axis. Gene. 2021;801:145855.
40. Kovalenko AA, Schwarz AP, Shcherbitskaia AD, Mikhel AV, Vasilev DS, Arutjunyan AV. Reference gene validation in the embryonic and postnatal brain in the rat hyperhomocysteinemia model. Neurotox Res. 2024;42(2):19.
41. Tanic N, Perovic M, Mladenovic A, Ruzdijic S, Kanazir S. Effects of aging, dietary restriction and glucocorticoid treatment on housekeeping gene expression in rat cortex and hippocampus-evaluation by real time RT-PCR. J Mol Neurosci. 2007;32(1):38–46.
42. Li B, Matter EK, Hoppert HT, Grayson BE, Seeley RJ, Sandoval DA. Identification of optimal reference genes for RT-qPCR in the rat hypothalamus and intestine for the study of obesity. Int J Obes (Lond). 2014;38(2):192–7.
43. Schwarz AP, Nikitina VA, Krytskaya DU, Shcherbakova KP, Trofimov AN. Reference gene expression stability within the rat brain under mild intermittent ketosis induced by supplementation with medium-chain triglycerides. PLoS ONE. 2023;18(2):e0273224.
44. Kraemer N, Neubert G, Issa L, Ninnemann O, Seiler AE, Kaindl AM. Reference genes in the developing murine brain and in differentiating embryonic stem cells. Neurol Res. 2012;34(7):664–8.
45. Cheung TT, Weston MK, Wilson MJ. Selection and evaluation of reference genes for analysis of mouse (Mus musculus) sex-dimorphic brain development. PeerJ. 2017;5:e2909.
46. Shaydurov VA, Kasianov A, Bolshakov AP. Analysis of housekeeping genes for Accurate normalization of qPCR Data during early postnatal Brain Development. J Mol Neurosci. 2018;64(3):431–9.
47. Sundaram VK, Sampathkumar NK, Massaad C, Grenier J. Optimal use of statistical methods to validate reference gene stability in longitudinal studies. PLoS ONE. 2019;14(7):e0219440.
48. Ho KH, Patrizi A. Assessment of common housekeeping genes as reference for gene expression studies using RT-qPCR in mouse choroid plexus. Sci Rep. 2021;11(1):3278.
49. Boda E, Pini A, Hoxha E, Parolisi R, Tempia F. Selection of reference genes for quantitative real-time RT-PCR studies in mouse brain. J Mol Neurosci. 2009;37(3):238–53.
50. Parikshak NN, Luo R, Zhang A, Won H, Lowe JK, Chandran V, Horvath S, Geschwind DH. Integrative functional genomic analyses implicate specific molecular pathways and circuits in autism. Cell. 2013;155(5):1008–21.
51. Willsey AJ, Sanders SJ, Li M, Dong S, Tebbenkamp AT, Muhle RA, Reilly SK, Lin L, Fertuzinhos S, Miller JA, et al. Coexpression networks implicate human midfetal deep cortical projection neurons in the pathogenesis of autism. Cell. 2013;155(5):997–1007.
52. Gulsuner S, Walsh T, Watts AC, Lee MK, Thornton AM, Casadei S, Rippey C, Shahin H, Consortium on the Genetics of S, Group PS, et al. Spatial and temporal mapping of de novo mutations in schizophrenia to a fetal prefrontal cortical network. Cell. 2013;154(3):518–29.
53. Li M, Santpere G, Imamura Kawasawa Y, Evgrafov OV, Gulden FO, Pochareddy S, Sunkin SM, Li Z, Shin Y, Zhu Y et al. Integrative functional genomic analysis of human brain development and neuropsychiatric risks. Science. 2018;362(6420).
54. Subramanian L, Calcagnotto ME, Paredes MF. Cortical malformations: lessons in Human Brain Development. Front Cell Neurosci. 2019;13:576.
55. Pfaffl MW, Tichopad A, Prgomet C, Neuvians TP. Determination of stable housekeeping genes, differentially regulated target genes and sample integrity: BestKeeper–Excel-based tool using pair-wise correlations. Biotechnol Lett. 2004;26(6):509–15.
56. Vandesompele J, De Preter K, Pattyn F, Poppe B, Van Roy N, De Paepe A, Speleman F. Accurate normalization of real-time quantitative RT-PCR data by geometric averaging of multiple internal control genes. Genome Biol. 2002;3(7):RESEARCH0034.
57. Andersen CL, Jensen JL, Orntoft TF. Normalization of real-time quantitative reverse transcription-PCR data: a model-based variance estimation approach to identify genes suited for normalization, applied to bladder and colon cancer data sets. Cancer Res. 2004;64(15):5245–50.
58. Silver N, Best S, Jiang J, Thein SL. Selection of housekeeping genes for gene expression studies in human reticulocytes using real-time PCR. BMC Mol Biol. 2006;7:33.
59. Xie F, Xiao P, Chen D, Xu L, Zhang B. miRDeepFinder: a miRNA analysis tool for deep sequencing of plant small RNAs. Plant Mol Biol. 2012;80(1):75-84.
60. Xie F, Wang J, Zhang B. RefFinder: a web-based tool for comprehensively analyzing and identifying reference genes. Funct Integr Genomics. 2023;23(2):125.
61. Bustin SA, Benes V, Garson JA, Hellemans J, Huggett J, Kubista M, Mueller R, Nolan T, Pfaffl MW, Shipley GL, et al. The MIQE guidelines: minimum information for publication of quantitative real-time PCR experiments. Clin Chem. 2009;55(4):611–22.
62. Bustin SA. Absolute quantification of mRNA using real-time reverse transcription polymerase chain reaction assays. J Mol Endocrinol. 2000;25(2):169–93.
63. Liu ZY, Tang F, Yang JZ, Chen X, Wang ZF, Li ZQ. The role of Beta2-Microglobulin in Central Nervous System Disease. Cell Mol Neurobiol. 2024;44(1):46.
64. Tristan C, Shahani N, Sedlak TW, Sawa A. The diverse functions of GAPDH: views from different subcellular compartments. Cell Signal. 2011;23(2):317–23.
65. Townsend MH, Robison RA, O'Neill KL. A review of HPRT and its emerging role in cancer. Med Oncol. 2018;35(6):89.
66. Cheever TR, Ervasti JM. Actin isoforms in neuronal development and function. Int Rev Cell Mol Biol. 2013;301:157–213.
67. Zhou X, Liao WJ, Liao JM, Liao P, Lu H. Ribosomal proteins: functions beyond the ribosome. J Mol Cell Biol. 2015;7(2):92–104.
68. Kraushar ML, Popovitchenko T, Volk NL, Rasin MR. The frontier of RNA metamorphosis and ribosome signature in neocortical development. Int J Dev Neurosci. 2016;55:131–9.

69. Harnett D, Ambrozkiewicz MC, Zinnall U, Rusanova A, Borisova E, Drescher AN, Couce-Iglesias M, Villamil G, Dannenberg R, Imami K, et al. A critical period of translational control during brain development at codon resolution. Nat Struct Mol Biol. 2022;29(12):1277–.
70. Loo L, Simon JM, Xing L, McCoy ES, Niehaus JK, Guo J, Anton ES, Zylka MJ. Single-cell transcriptomic analysis of mouse neocortical development. Nat Commun. 2019;10(1):134.
71. Di Bella DJ, Habibi E, Stickels RR, Scalia G, Brown J, Yadollahpour P, Yang SM, Abbate C, Biancalani T, Macosko EZ, et al. Molecular logic of cellular diversification in the mouse cerebral cortex. Nature. 2021;595(7868):554–9.

Publisher's note